Human Behavioral Metrics of a Predictive Model Emerging During Robot Assisted Following Without Visual Feedback

Anuradha Ranasinghe[1], Prokar Dasgupta[2], Atulya Nagar[1], and Thrishantha Nanayakkara [3]

***Abstract*—Robot assisted guiding is gaining increased interest due to many applications involving moving in noisy and low visibility environments. In such cases, haptic feedback is the most effective medium to communicate. In this paper, we focus on perturbation based haptic feedback due to applications like guide dogs for visually impaired people and potential robotic counterparts providing haptic feedback via reins to assist indoor firefighting in thick smoke. Since proprioceptive sensors like spindles and tendons are part of the muscles involved in the perturbation, haptic perception becomes a coupled phenomenon with spontaneous reflex muscle activity. The nature of this interplay and how the model based sensory-motor integration evolves during haptic based guiding is not well understood yet. In this study, we asked human followers to hold the handle of a hard rein attached to a 1-DoF robotic arm that gave perturbations to the hand to correct an angle error of the follower. We found that human followers start with a 2^{nd} order reactive autoregressive following model and changes it to a predictive model with training. The post-perturbation Electromyography (EMG) activity exhibited a reduction in co-contraction of muscles with training. This was accompanied by a reduction in the leftward/rightward asymmetry of a set of followers behavioural metrics. These results show that the model based prediction accounts for the internal coupling between proprioception and muscle activity during perturbation responses. Furthermore, the results provide a firm foundation and measurement metrics to design and evaluate robot assisted haptic guiding of humans in low visibility environments.**

***Index Terms*—Haptics, Human-robot interactions, behavioural metrics.**

I. INTRODUCTION

In the case of human intervention in disaster response operations like indoor fire fighting where the environment perception is limited due to thick smoke, noise in the Oxygen masks, and clutter, impairment of environmental perception compounds distress. Haptic mode of communition offers a good solution because it is the least affected perception in such cases. Our previous studies using human-human demonstrations of haptic based guidance using a hard rein showed that the guiders build a 3rd order predictive autoregressive model whereas the naive blindfolded followers exhibit a 2nd order reactive autoregressive model [1], [2]. In this paper we implemented the identified predictive guiance policy on a 1-DoF robotic arm to understand the interplay between muscle activity and haptic perception and how model based sensorimotor integration evolves during training.

Robotic guidance has been addressed in several physical Human-Robot Interaction (HRI) scenarios such as search and rescue, disaster response [3], human navigation [4], [5], [6], and even during dance training [7]. In [8], authors report a number of cases where computer controlled mechatronic devices are used to provide remote haptic perception of real environments. A human with perceptual limitations due to physiological or environmental reasons would regain smooth movements with guiding assistance. A robotic guide dog called Rovi [9] to guide a human with limited environment perceptions is an example.

When a robot guides a human in a low visibility environment using arm perturbations, it is important to understand how humans perceive the arm perturbation. There are several metrics used to assess the effectiveness of human-robot interactions [10], [11]. In [10] authors present analysis of human-robot co-operative load transport to adjust the robot's urge to complete the task based on the human feedback. In this study, the authors introduce metrics that quantify mass and grasp. Moreover, the study to understand the interaction patterns involving two or more humans in the physical task, a confusion matrix was used to classify some behavioural patterns [11]. Studies done in morphological computation [12] show that perception and action are related through a shared embodiment [13], [14]. When haptic perception is coupled with muscle activation due their shared embodiment, the brain is posed with the challenge of compensating for asymmetries in perception of equal perturbations given in different directions due to inherent asymmetry in muscle activation.

In this study, experiments were designed to understand humans' perception of external perturbations on the resting hand. We implemented a previously identified 3^{rd} order guiding control policy on a planar 1-DoF robotic arm to guide blindfolded subjects to reach a desired point. This paper presents two experiments. The first experiment attempts to study any symmetry in behavioural metrics such as Rise Time (RT), best fit model order of the polynomial fitted to the instantaneous error of the human's position for a given desired angle (N), and Steady State Variability (SSV) when the extracted guiding control policy in human demonstration experiments was implemented on a planar 1-DoF robotic arm to

Manuscript received: October 07, 2017; Revised January 11, 2018; Accepted; March 01,2018.

This paper was recommeneded for publication by Editor Yasuyoshi Yokokohji upon evealuation of the Associate Editor and Reviewers' comments

This work was supported in part by the U.K. Engineering and Physical Sciences Research Council (EPSRC) under Grants: EP/M506357/1, EP/I028757/1 and EP/N03211X/2, the Guy's and St Thomas' Charity: grant no. R090705, Higher Education Innovation Fund (HEIF), and Vattikuti foundation

[1]Anuradha Ranasinghe and Atulya Nagar are with Department of Mathematics and Computer Science, Liverpool Hope University, United Kingdom, dissana,nagara@hope.ac.uk

[2]Prokar Dasgupta is with MRC Centre for Transplantation, DTIMB & NIHR BRC, Kings College London, United Kingdom, prokar.dasgupta@kcl.ac.uk

[3]Thrishantha Nanayakkara is with Dyson School of Design Engineering, Imperial College London, United Kingdom. t.nanayakkara@imperial.ac.uk

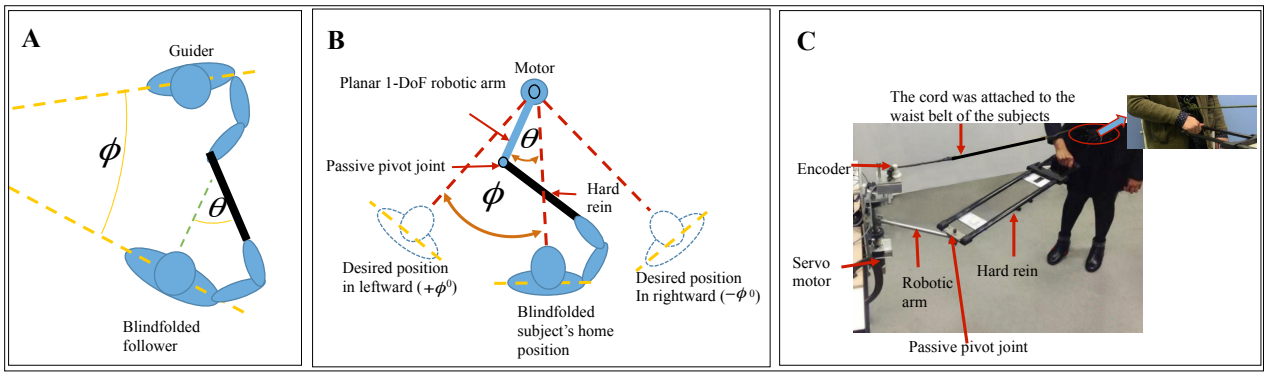

Fig. 1: Experiment 1: Experimental set up, A) The diagram for human-human demonstration (the guider and follower duo) in our previous studies [1], [2]: the state is ϕ and the action is θ. ϕ is the orientation difference between the guider and the follower and θ is angle of the rein relative to the agent, B) The schematic diagram of human-robot interaction: The guiding policy, extracted from human demonstrations in [1], [2] shown in Fig. 1A was implemented on the planar 1-DoF robotic arm, and C) Human-robot experimental setup: The cord was attached to the waist belt of the blindfolded subjects and the encoder on the robot to measure the relative error between the human and the motor shaft (ϕ).

perturb the blindfolded subjects' most dominant arm to guide them in leftward/rightward directions. Next, the experiment 2 was designed to study muscle activation just after the arm perturbation.

The structure of the rest of the paper is as follows. Section II elaborates the experimental methodology to collect data of subjects. Section III gives the experimental results of subjects. Finally, section IV gives a conclusion and future works.

II. Experimental Methodology

A. Experimental protocol: human-robot interactions

In both experiments, the subjects were given the Oldfield 1971 handedness questionnaire [15] to avoid adding ambidextrous in to the analysis. Visual feedback to the subject was cut off by blindfolding, while the auditory feedback was cut off by playing a sound track of less than 70 dB (For example noise in a cocktail party). The experimental protocol was approved by the King's College London Biomedical Sciences, Medicine, Dentistry and Natural & Mathematical Sciences research ethics committee.

Subjects were given an arm perturbation by a planar 1-DoF robotic arm. Therefore, subjects' movements were limited to leftward and rightward movements from the home position (the home position is shown in Fig. 1B). Leftward and rightward angular position from home position were taken as $+\phi^\circ$ and $-\phi^\circ$ respectively (Hereafter, $+\phi^\circ$ and $-\phi^\circ$ notation will be used to leftward and rightward movements throughout this paper). Since the robotic arm was mounted on a stationary table, the subjects' movement was limited to maximum 90° and -90° angles in leftward and rightward movements. Therefore, $\pm 65^\circ$ and $\pm 25^\circ$ were taken as maximum and minimum desired angles to represent large and small initial errors to be corrected by the robotic guider.

B. Experimental setup

The schematic diagram of replication of human-human experiments in our previous studies in Fig. 1A were replicated by human-robot experiments as shown in Fig. 1B. In Fig. 1B, the angle (ϕ) is the error of following (The angle between the human's current position and the desired position around the motor axis), the angle (θ) is the robotic arm's swing angle on the horizontal plane. Moreover, the replicated physical experimental setup is shown in Fig. 1C. In Fig. 1C, the guider's arm was replaced by planar 1-DoF robotic arm to generate the swing arm action in horizontal plane. The cord was attached to the waist belt of the blindfolded subject and the encoder on the robot arm to measure the error between the human and the desired position (ϕ). The planar robot arm shaft was driven by a Maxon EC60 (ϕ) mm brush less 400 Watt with Hall sensors motor. An EPOS2 50/5 digital position controller was used to control the motor. Here, NI LabVIEW 2009 was used for programming and communicating with other hardware devices to control the robotic arm. The joint between the robotic arm and the hard rein was a passive joint to behave like a guider's arm in human-human interaction experiments in Fig. 1A. The other end of the hard rein was held by the human follower as shown in Fig. 1C.

C. Subject's training phase

Before starting the experimental trials, subjects were trained to give an idea to move proportional to the given tug force. For the training, the desired angles were chosen different from experimental angles such as $-10^\circ, -20^\circ, -30^\circ, +10^\circ, +20^\circ$, and $+30^\circ$. Blindfolded subjects were asked to follow the arm perturbation without manipulating any force and step to the new position from the initial position of the subject. Here, the planar robot arm perturbed subject's most dominant arm with a single tug force in the direction of the desired movement. The subjects performed 5 trials for each training angle. In the training phase, the subjects were trained to move proportional to the perturbed tug force.

D. Experimental procedure

Experiment 1 and experiment 2 procedures are as follows.

1) Experiment 1: Study the humans' behavior in human-robot interaction: Eight (4-male, 4-female) naive and ten (5-male, 5-female) trained right-handed subjects participated in the experiment after giving informed consent for the experiment 1. They were healthy and in the age group of 21 - 30 years. In any given trial, subjects started to move from the home position to the direction of the arm perturbation as shown Fig. 1B. Subjects were instructed to move proportional to the force they felt and to the direction of the tug force. The instantaneous error of the follower's position relative to a desired angle (ϕ) was recorded by an encoder (Rotary encoder SP Series: SP115669-360PPR).

Once the trial was started, the encoder read instantaneous error of the follower's position relative to a desired angle (ϕ). Then the robotic arm computed the commands to minimise the error between the human subject and the desired angle within the 70s time based on the control policy we previously indentified in [2]. During that time, 23 action commands (iterations) were recorded. For a given desired angle, same trial was repeated three times. Therefore, eighteen trials were recorded during the experiment. Subjects were given a five minutes break after every six trials to minimise fatigue. In this experiment, we defined six desired angles (ϕ): $-25°, -45°, -65°, +25°, +45°$, and $+65°$. The order of the reaching desired angles was selected pseudo randomly and it was maintained consistently across all subjects.

2) Experiment 2: Study humans' arm muscle spontaneous responses immediately after the arm's perturbation: Five naive subjects (2-male, 3-female) and ten (6-male, 4-female) trained subjects participated to the experiment 2. They were healthy and in the age group of 21 - 28 years. The Experiment 2 was conducted to study humans' arm muscle responses when the subject's arm is perturbed from leftward/rightward directions. For simplicity, $-45°$ and $+45°$ were taken as the desired angular positions and the subject's most dominant arm was perturbed by a single tug to study arm muscles actuation immediately after the arm perturbation. Five trials were recorded for each desired angles.

Surface EMGs were recorded by using the EMG (Noraxon, USA) sensors from the following muscles of the blindfolded subject's most dominant arm: Anterior Deltoid(AD), Posterior Deltoid (PD), Biceps (Bc), Median Triceps (MT), Brachioradialis (Br), Flexor Carpi Radialis (FCR), Extensor Carpi Ulnaris (ECU), and Extensor Carpi Radialis (ECR). Before attaching EMG electrodes, the skin was cleaned with alcohol. The electrodes were 2 mm in diameter and 12 mm apart. EMG records were carefully monitored for stimulus artefacts, noise, and cross-talk by firmly attaching to the skin using double-sided adhesive tape.

III. Results

A. Model nature of the human follower in human-robot experiments

Since the follower's model order and the nature (reactive/predictive) were extracted in our previous human demonstration experiments when the blindfolded human is guided by another human via a hard rein, it would be interesting to test the subjects' model order and the nature in HRI. In our previous experiments [2], it was found that on average the naive follower used a 2^{nd} order reactive model. Here, our aim is to find out whether this would change with training for the same guiding control algorithm.

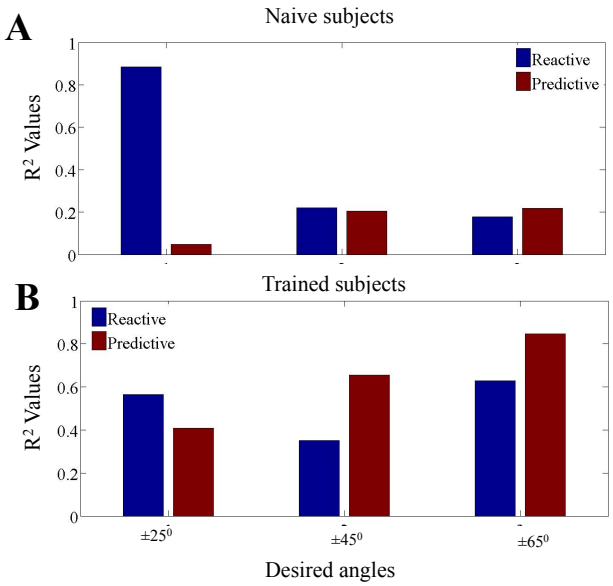

Fig. 2: Experiment 1: Reactive and predictive model nature (reactive/predictive) in reaching desired angles of $\pm 65°$, $\pm 45°$, and $\pm 25°$:A) Average R^2 for naive subjects' model nature, and B) Average R^2 for trained subjects' model nature.

	Naive Subjects		TrainedSubjects	
	Reactive	Predictive	Reactive	Predictive
$\pm 25°$	0.281	-0.041	-0.118	0.0295
$\pm 45°$	0.190	-0.0489	-0.46	0.054
$\pm 65°$	-0.046	0.092	-0.042	0.067

TABLE I: Experiment 1: The gradient of R^2 values of reactive and predictive models in reaching $\pm 65°$, $\pm 45°$, and $\pm 25°$ desired angles over trials.

1) Modeling the follower's state transition policy : Here we revisited the mathematical methods that we have been used in our previous studies to find the model nature. First, we show the brief description of the method that we have used in our previous studies [1], [2].

We model the follower's state transition policy by an Auto-Regressive model (AR) as an N-th order discrete linear controller. AR model gives us temporal (model nature) and structural (model order) relationship. Our first attempt is to find the model nature of the follower. Here, the order N depends on the number of past states used to calculate the current action. Let the state be the relative orientation between the guider and the follower given by ϕ, and the action be the angle of the rein relative to the sensor on the chest of the guider given by θ as shown in Fig. 1A. We model the follower's state transition policy as an N-th order action dependent discrete linear controller to understand behaviour of the follower. The order N depends on the number of past actions used to

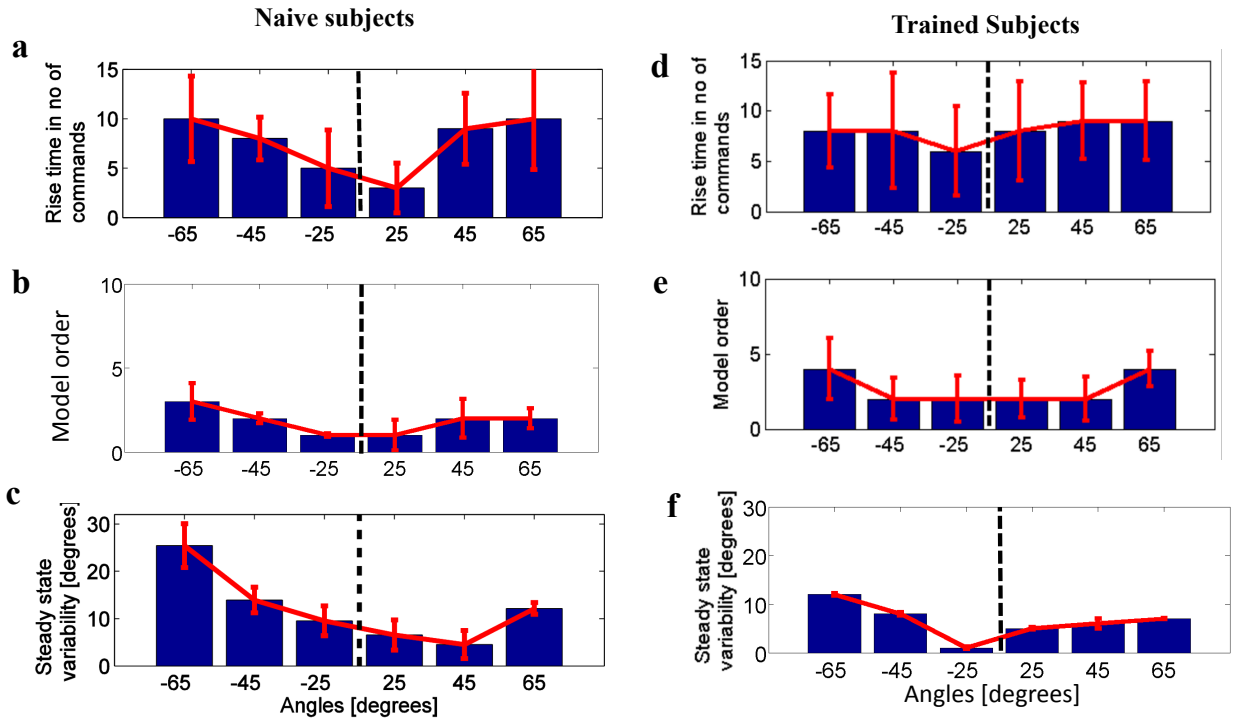

Fig. 3: Experiment 1: The behavioural metrics for reaching six desired angles for naive and trained subjects: a) Average Rise time (RT) for naive subjects in transient response, b) Average Model order (N) for naive subjects: the best fit model order is set by AIC, c) The average Steady State Variability (SSV) for reaching six desired angles across all naive subjects, d) Average RT for trained subjects in transient response, e) Average N for trained subjects, and f) Average SSV for reaching six desired angles across all trained subjects. The black dashed line is to show the home position and standard error is shown by red with error bars from Fig. 3a to Fig. 3f.

calculate the current state. Then the linear discrete control policy of the follower is given by

$$\phi_f(k) = \sum_{r=0}^{N-1} a_r^{fRe}\theta_f(k-r) + c^{fRe} \tag{1}$$

if it is a reactive controller, and

$$\phi_f(k) = \sum_{r=0}^{N-1} a_r^{fPre}\theta_f(k+r) + c^{fPre} \tag{2}$$

If it is a predictive controller, where, k denotes the sampling step, N is the order of the polynomial, $a_r^{Re}, a_r^{Pre}, r = 0, 1, 2, \cdots, N-1$ is the polynomial coefficient corresponding to the r-th state in the reactive and predictive model respectively, and c^{Re}, c^{Pre} are corresponding scalars. These linear controllers can be regressed with the experimental data obtained the R^2 values (coefficient of determination). The behaviour of these coefficients for all human subjects across the learning trials will give us useful insights as to the predictive/reactive nature of the control policy. First Eq. 1 Eq. 2 were regressed to find the Coefficients of equations (1) and (2) for reaching six desired angles ($\pm 65°$, $\pm 45°$, and $\pm 25°$).

Here the Eq. 1 and Eq. 2 were used to find the R^2 values for reactive and predictive models respectively. We use the R^2 value to quantify the fraction of the variation of experimental data explained by the fitted model. i.e. If R^2 value is 0.9, the model explains 90% of the experimental relationship between the dependent and independent variables. Therefore, an increase in the R^2 value for a predictive model across trials means that the followers' behavior increasingly become a predictive policy (a map from inputs (robot's commands) to outputs (movement)).

To test that, the gradient of R^2 values of reactive and predictive models in reaching $\pm 65°$, $\pm 45°$, and $\pm 25°$ desired angles over trials are shown in Table. I. Polyfit in Polynomial curve fitting (MATLAB 2014a) was used to fit the linear curves to find the gradients. On average the positive trend in reactive model in naive subjects shows that, naive subjects emphasize more on reactive than predictive following behaviors. However, after training the positive gradient for predictive model shows that trained subjects give more emphasis on predictive nature than reactive as shown in Table. I. Moreover, by selecting reactive/predictive nature, we summarize the model nature in reaching $\pm 65°$, $\pm 45°$, and $\pm 25°$ desired angles for naive and trained in Fig. 2A and Fig. 2B respectively. In general, there were not much improvement in R^2 values for naive subjects as shown in Fig. 2A. However, R^2 values in 2B for trained subjects were improved. Both naive and trained subjects have mixed reactive and predictive nature in reaching

desired angles as shown in Fig. 2. However, naive subjects have more dominant reactive nature as shown in Fig. 2A. Interestingly trained subjects' most dominant model nature is predictive as shown in Fig. 2B. From the fact that all subjects use a mixed strategy with an increasing bias to use a predictive approach with training, we can also deduce that whenever possible, subjects take a predictive approach even before the training. For example, naive and trained subjects show more predicting model nature moving to $\pm 65^{\circ}$ as shown in Fig. 2. However, they become more predictive for all error correction levels after training and is more pronounced in reaching higher angles as shown in Fig. 2B. In general, the results in Fig. 2 show that subjects have intrinsic tendency to be predictive when ever possible.

Therefore the results show that the predictive nature is more dominant than reactive after training. In general, naive subjects' dominant model nature is reactive and they have a mixed model nature before and after training phase. The model nature changes could come from various reasons. Next we are interested to test the possible causes for the model nature changes after the training. To test that, we move into study subjects' behaviour in reaching six desired angles.

B. Experiment 1: behavioral metrics in left and right arm perturbations

Here, we present the behavioural metrics such as Rise Time (RT), best fit model order of the polynomial fitted to the instantaneous error of the humans' position for a given desired angle (N), and Steady State Variability (SSV) for naive and trained subjects to understand how those metrics relate with subjects model nature selection strategies. We are interested to test whether subjects are going to optimize their behavioural metrics RT, N, or SSV in reaching.

1) Rise time (RT): Here we are interested to see how fast the human subject could respond and settle down in the desired angular position in transient response for naive and trained subjects as shown in Fig. 3a and Fig. 3d respectively. In this regard, the RT is considered as measured number of robotic arm commands to reach from 10% to 90% of the desired angles. We see that average rise time increases with training. This can come from a predictive model that develops a critically damped response as opposed to a fast reactive response with higher settling time.

2) Model order (N): Here Akaike Information Criterion (AIC) is used to find the best fit order of the reaching curves of the polynomials [16] as shown in Fig. 3b and Fig. 3e for naive and trained subjects respectively. The results show that the follower's behaviour fits a 2^{nd} order polynomial when the desired angles are -25°, and $+25^{\circ}$ for the naive subjects and -45°, -25°, $+25^{\circ}$, and $+45^{\circ}$ for the trained subjects as we observed in human demonstration experiments for the follower. Therefore, the test results shows that when the subjects are trained, the model order is more consistent as shown in Fig. 3e.

3) Steady State Variability (SSV): For a stable controller, steady state response should be as close as possible to the desired angular position. Therefore, the last 10% (steady state) of experimental recordings of the instantaneous error of the subject's position relative to the desired angle/target point (ϕ) is taken for steady state analysis as shown in Fig. 3c and Fig. 3f for naive and trained subjects respectively. The naive subjects' steady state variability is comparatively high as shown in Fig. 3c. However, after training subjects were able to bring low steady state variability in reaching desired angles as shown in Fig. 3f. Moreover, standard error reduction in reaching is noticed in Fig. 3f for trained subjects for SSV. This again confirms damped nature in moving without overshooting. This smoothness in settling is characteristic of a internal model based predictive movement [17], [18].

Next, we moved to test whether there is a behavioural symmetry in moving leftward and rightward directions after arm perturbation in RT, N, and SSV. The ratio in moving leftward/rightward directions in reaching desired angles for RT, N, and SSV were taken. Our argument is, if the subjects move leftward and rightward symmetrically, the ratio, M ≈ 1. The average ratios (M) and Standard deviation (STD) of ratios are shown in Table II. However, none of the M values in RT, N, and SSV are equal to 1. Since the distributions of behavioural metrics are not symmetric, one tailed t-test was performed to test whether there is a statistically significant difference between the distribution of each metric in leftward vs rightward movements. We used a significance level of $P = 0.05$. Table II shows that the behavioural metrics in leftward and rightward movements are asymmetric ($P < 0.05$ for the null hypothesis that M is not equal to 1). The M and P values in Table II show that the asymmetry in moving leftward/ rightward directions (M $\neq 1$, and P $\nleq 0.05$). Moreover, it is noticed that there is a reduction in that asymmetry when subjects are trained as shown in Table II by *. Here, all significance values for trained behavioural metrics are dropped as shown in Table II. The possible cause for the drop of significance values for the trained subjects could come from subjects being predictive after the training. Next we move on to study the subjects' arm muscle activation just after the arm perturbation to test if there is any significance difference in muscle activation in leftward/rightward arm perturbation.

C. Experiment 2: Spontaneous muscle response immediately after the given a single tug

The experiment 2 was conducted to test whether the asymmetry of perception noticed in behavioural metrics come from different activation of muscles in leftward and rightward arm perturbation, based on the hypothesis that haptic perception depends on how muscles are activated by restoring reflex after the perturbation. When the arm is perturbed, the muscle lengthens and muscle spindles are stretched. This contraction in muscle tension provides different degrees of pull on the tendon. Therefore, arm muscles' spontaneous responses were tested in EMG in experiment 2 immediately after the arm perturbation (Note that, in this experiment a right-handed group different from experiment 1 have participated to the experiment 2).

EMG is a non-invasive method to quantify the relationship between a specific movement and the activation of the

		Desired Angles		
		25°	45°	65°
Rise Time (RT)	N	M: 0.648 STD: 0.421 P: 0.316	M: 0.672 STD: 0.167 P: 0.931	M: 0. 674 STD: 0.200 P: 0.559
	T	M: 0.532 STD: 0.302 P: 0.157*	M: 0.454 STD: 0.225 P: 0.852*	M: 0. 690 STD: 0.170 P: 0.417*
Model order (N)	N	M: 0.666 STD: 0.516 P: 0.858	M: 0.550 STD: 0.300 P: 0.467	M: 0. 666 STD: 0.408 P: 0.619
	T	M: 0.570 STD: 0.476 P: 0.174*	M: 0.696 STD: 0.330 P: 0.253*	M: 0. 625 STD: 0.252 P: 0.181*
Steady State Variability (SSV)	N	M: 0.568 STD: 0.278 P: 0.749	M: 0.509 STD: 0.307 P: 0.786	M: 0. 614 STD: 0.274 P: 0.184
	T	M: 0.562 STD: 0.293 P: 0.701*	M: 0.399 STD: 0.312 P: 0.744*	M: 0. 485 STD: 0.242 P: 0.109*

TABLE II: Experiment 1: The asymmetry testing: M: the average ratio reaching desired angles in leftward/rightward directions, STD: the average standard deviation of the M, and P: p value of the significance rest results for moving leftward and rightward in desired angles (one tailed t test) for behavioural metrics RT, N, and SSV for Naive (N) and Trained (T) subjects.

underlying muscle groups. Therefore, the EMG signals in arm flexion/extension just after the single arm perturbation were studied in moving 45° in leftward/rightward directions as shown in Fig. 4A. Since arm muscles are activated differently, the EMG recordings were normalized as shown in Fig. 4B and 4C for naive and trained subjects respectively. The normalized average total number of peaks occurred during the arm flexion/extension is presented in Fig. 4B and Fig. 4C for naive and trained subjects respectively. Our method was consisted with other research [19] that focused on peaks in EMG to study limb patterns during the multi-joint movements. Here, EMG recording across the arm muscles of Anterior Deltoid (AD), Posterior Deltoid (PD), Biceps (Bc), Median Triceps (MT), Brachioradialis (Br), Flexor Carpi Radialis (FCR), Extensor Carpi Ulnaris (ECU), and Extensor Carpi Radialis (ECR) in anti clock wise direction across all subjects. Butterworth filter (MATLAB 2012b) was used for subtracting noise from low magnitude surface EMG [20].

In general, the total number of peaks occurred in flexion and extension are different as shown in Fig. 4B and Fig. 4C for naive and trained subjects. Since the data are not normally distributed, the Mann-Whitney U test was used to test the significance in arm flexion and extension. Significance was noticed between arm flexion and extension for both naive ($p = 0.0172$) and trained ($p = 0.0001$) subjects. The results show that on average the muscle activation is significantly different just after the leftward/rightward arm perturbations. Moreover, the drop in p-values significance from naive to trained subjects again confirm reduction in muscle co-contraction due to the predictive model after training. Therefore, the results confirm that asymmetry in behavioural metrics could accompany difference in muscle activation as noticed in Fig. 4. Therefore, we conclude that the drop in the behavioural asymmetry could come from the reduction in muscle co-contraction due to the predictive model.

Next, we tested what behavioral criteria subjects try to optimize by being predictive in reaching desired angles as shown Fig. 2. To test that, the behavioural metrics RT, N, and SSV results were compared to reaching -65°, -45°, -25°, $+25^\circ$, $+45^\circ$, and $+65^\circ$ for naive and trained subjects as shown in Fig. 3. Interestingly, trained subjects take more time than naive subjects as shown in Fig. 3d and Fig. 3a respectively. The higher RT comes from damped reaction and lower RT comes from undamped reaction with overshooting. Moreover, after training, a consistent model order ($N = 2$) was noticed in trained subjects in Fig. 3e. The higher RT, and model consistency after training could come from steady movements of the subjects than overshooting in undamped movements. Furthermore, the SSV variability is reduced after the training for reaching all desired angles as shown in Fig. 3f. Therefore, in summary the results in behavioural metrics show that by being predictive, subjects achieve higher RT, lower SSV, and consistent model order (N) after training whereas naive subjects have inconsistent model order, higher SSV, and lower RT as shown Fig. 3.

IV. Conclusion

This paper presents metrics that can be used to monitor the change of control mechanisms of human followers during haptic-based guidance training. Experimental results show that the subjects develop a predictive behavior accompanied by a reduction in muscle co-contraction with training. This taken together with the reduction in the asymmetry of behavioral indexes show that the model based prediction accounts for the internal coupling between proprioception and muscle activity during perturbation responses. These findings provide a valuable basis to design training protocols for robot assisted guiding. Theoretical and psychophysical studies in reaching movements have suggested that humans learn novel dynamic environments by building specific internal models in reaching movements symbolized by improved smoothness of movements and reduction in muscle co-contraction [17], [18].

Our results on the asymmetry of behavioural indexes together with difference in muscle activation patterns for the

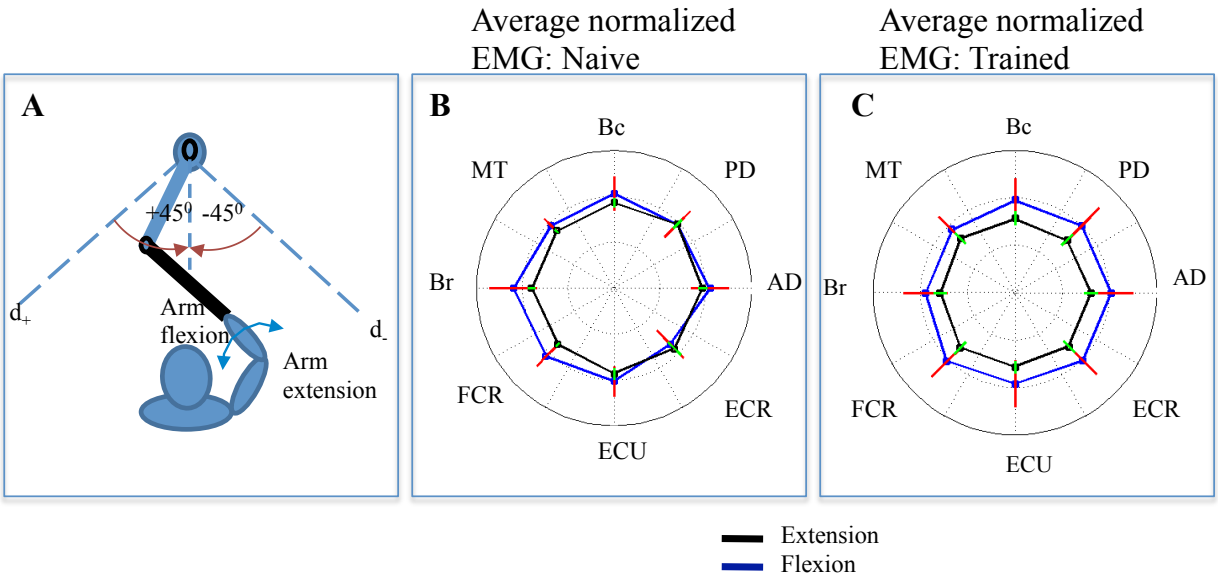

Fig. 4: Experiment 2: A) Experimental set up. The desired angle is $45°$ in leftward and rightward directions from the home position, B) Naive subjects' EMG activation: The average normalized total number of peaks occurred in EMG recordings across all naive subjects for eight different arm muscles, and C) Trained subjects' EMG activation. Here the average normalized total number of peaks occurred in EMG recordings across all trained subjects for eight different arm muscles, in Fig. 4B and Fig. 4C, the extension and flexion of the arm are shown by blue and brown colours respectively. The standard error for extension and flexion are shown by black and red. The arm muscles were chosen as Anterior Deltoid(AD), Posterior Deltoid (PD), Biceps (Bc), Median Triceps (MT), Bra- chioradialis (Br), Flexor Carpi Radialis (FCR), Extensor Carpi Ulnaris (ECU), and Extensor Carpi Radialis (ECR).

perturbations given in leftwards vs rightwards show that perception of external perturbations are coupled with the resulting spontaneous muscle activation reflexes. When the arm is perturbed the muscle lengthens and muscle spindle is stretched. This contraction in muscle tension provides different degrees of pull on the tendon in the arm muscles of the humans. Therefore, in the experiment 2, we hypothesize that haptic perception depends on how muscles are activated by restoring reflex after the arm perturbation. Since a significant difference was noticed in arm flexion and extension for both naive ($p = 0.0172$) and trained ($p = 0.0001$) subjects and the drop in the difference of EMG between extension/flexion from naive to trained subjects, here we conclude that the drop in EMG could come from reduction in muscle co-contraction due to the predictive model. Recent studies on manual soft tissue palpation to identify hard nodules have found that human subjects use muscle co-contraction variation to gain haptic information [21]. Experiments on soft robotic counterparts to do the same palpation task have found that stiffness control in the body in fact plays an important role in uncertainty reduction in haptic perception [22]. The findings in this paper further confirm that muscle co-contraction and haptic perception are intrinsically coupled. Moreover, we found that development of model based predictive control with training help to reduce asymetry of perception present in naive subjects by reducing antagonistic muscle co-contraction to develop a more isotropic post-perturbation spontaneous muscle activation. Therefore, to the best of our knowledge, this is the first time to report that training leads to changes in both perception and muscle activation. Therefore, the experimental findings reported in this paper provide new evidence to show the importance of treating perception and action as a coupled phenomenon [23] in living beings that cannot be easily separated as often practiced in traditional control theory.

The new insights into how physical embodiment, the common infrastructure to perception and action in living beings, enables us to design better robotic systems that interact with human counterparts using physical perturbations. The behavioral metrics presented in this paper to quantify the effect of model based predictive controllers will also provide a new basis to monitor the quality of training in a human-robot interaction scenario. One candidate application is haptic-based guidance via a hard rein in low visibility conditions such as in-door fire fighting and disaster response applications.

References

[1] A. Ranasinghe, J. Penders, P. Dasgupta, K. Althoefer, & T. Nanayakkara, "*A two party haptic guidance controller via a hard rein*", 2013 IEEE/RSJ International Conference on in Intelligent Robots and Systems (IROS), pp. 116-122, 2003.

[2] A. Ranasinghe, J. Penders, P. Dasgupta, K. Althoefer, & T. Nanayakkara, "*Identification of haptic based guiding using hard reins*", PloS one 10, vol. no. 7, e0132020, 2015.

[3] J. Casper, & R. Murphy, "*Human-robot interactions during the robot-assisted urban search and rescue response at the world trade center*", IEEE Transactions on Systems, Man, and Cybernetics, Part B (Cybernetics), 33(3), pp. 367-385. 2003.

[4] J. Loomis, R. . Golledge, R. Klatzky, & J. Marston, "*Assisting wayfind- ing in visually impaired travelers*", Applied spatial cognition: From research to cog- nitive technology, pp. 179-202, 2007.

[5] V. Kulyukin, C. Gharpure, J. Nicholson, & S. Pavithran, "*Rfid in robot-assisted indoor navigation for the visually impaired*," IEEE/RSJ International Conference on in Intelligent Robots and Systems (IROS), vol. 2, pp. 1979 1984, 2004.

[6] J. Campbell, R. Sukthankar, & I. Nourbakhsh, "*Techniques for evaluating optical flow for visual odometry in extreme terrain*, IEEE/RSJ International Conference on in Intelligent Robots and Systems (IROS), vol. 4, pp. 3704-3711, IEEE, 2004.

[7] D. Granados, J. Kinugawa, Y. Hirata, & K. Kosuge,. "*Guiding human motions in physical human-robot interaction through COM motion control of a dance teaching robot*", IEEE-RAS 16th International Conference on In Humanoid Robots (Humanoids), pp. 279-285, 2016.

[8] Vladareanu, Luige, et al., "*Haptic interfaces for the rescue walking robots motion in the disaster areas"*, Control (CONTROL) UKACC International Conference on. IEEE, 2014.

[9] M. Allan, B. Prabu, R. Nagarajan, & I. Bukhari, "*ROVI: a robot for visually impaired for collision- free navigation*, Proc. of the International Conference on Man-Machine Systems (ICoMMS 2009), pp. 3B5-1-3B5-6, 2009.

[10] Mrtl, Alexander, Martin Lawitzky, Ayse Kucukyilmaz, Metin Sezgin, Cagatay Basdogan, & Sandra Hirche. "The role of roles: Physical cooperation between humans and robots." The International Journal of Robotics Research 31, no. 13 (2012): 1656-1674.

[11] Madan, Cigil Ece, Ayse Kucukyilmaz, Tevfik Metin Sezgin, & Cagatay Basdogan. "Recognition of haptic interaction patterns in dyadic joint object manipulation." IEEE transactions on haptics 8, no. 1 (2015): 54-66.

[12] Guaman, S. A. A., Sornkarn, N., Nanayakkara, T. The role of morphological computation of the goat hoof in slip reduction, 2016 IEEE/RSJ International Conference on Intelligent Robots and Systems (IROS), pp. 5599 5605

[13] Iida, F. and Nurzaman, S.G., 2016. Adaptation of sensor morphology: an integrative view of perception from biologically inspired robotics perspective. Interface focus, 6(4), p.20160016.

[14] Chathuranga, D. S., Wang, Z., Noh, Y., Nanayakkara, T., Hirai, S., A Soft Three Axis Force Sensors that is Useful for Robot Grippers, 2016 IEEE/RSJ International Conference on Intelligent Robots and Systems (IROS), pp. 5556 5563

[15] R. Oldfield, "*The assessment and analysis of handedness*", The edinburgh inventory, Neuropsychologia, vol. 9, no. 1, pp. 97-113, 1971.

[16] H. Akaike, "*A new look at the statistical model identification*", IEEE Transactions on Automatic Control, vol. 19, no. 6, pp. 716-723, 1974.

[17] K Thoroughman, "*Human Motor Learning in Stationary and Nonstationary Novel Dynamic Environments: Psychophysical, Electromyographic, and Computational Verification and Extension of the Inverse Model Hypothesis*, Ph.D. dissertation, The Johns Hopkins University, Baltimore, Maryland, 1999.

[18] K Thoroughman, &, R Shadmehr. "*Electromyographic correlates of learning an internal model of reaching movements*" Journal of Neuroscience, 19.19, pp. 8573-8588, 1999.

[19] P. Gribble, D. Ostry, V. Sanguineti, & R. Laboissiere, "*Are complex control signals required for human arm movement*", Journal of Neurophysiology, vol. 79, no. 3, pp. 1409-1424, 1998.

[20] R. Mello, L. Oliveira, & J. Nadal, "*Digital butterworth filter for subtracting noise from low magnitude surface electromyogram*", Journal of Computer methods and programs in biomedicine, vol. 87, no. 1, pp. 28-35, 2007.

[21] Sornkarn, N. and Nanayakkara, T., 2017. Can a soft robotic probe use stiffness control like a human finger to improve efficacy of haptic perception?. IEEE transactions on haptics, 10(2), pp.183-195.

[22] Sornkarn N, Dasgupta P, Nanayakkara T (2016) Morphological Computation of Haptic Perception of a Controllable Stiffness Probe. PLoS ONE 11(6): e0156982.

[23] Pfeifer, R., Iida, F. and Gmez, G., 2006, June. Morphological computation for adaptive behavior and cognition. In International Congress Series (Vol. 1291, pp. 22-29). Elsevier.